THE JOURNAL OF PHYSICAL CHEMISTRY Letters

Letter

pubs.acs.org/JPCL

Single-Crystal Pentacene Valence-Band Dispersion and Its Temperature Dependence

Yasuo Nakayama,*[,†] Yuta Mizuno,[‡] Masataka Hikasa,[†] Masayuki Yamamoto,[‡] Masaharu Matsunami,[§] Shinichiro Ideta,[§] Kiyohisa Tanaka,[§] Hisao Ishii,[‡,∥] and Nobuo Ueno[‡]

[†]Department of Pure and Applied Chemistry, Graduate School of Science and Technology, Tokyo University of Science, 2641 Yamazaki, Noda 278-8510, Japan

[‡]Graduate School of Advanced Integration Science, Chiba University, 1-33 Yayoi-cho, Inage-ku, Chiba 263-8522, Japan

[§]UVSOR Facility, Institute for Molecular Science (IMS), National Institutes of Natural Sciences, 38 Nishigo-Naka, Myodaiji, Okazaki 444-8585, Japan

[∥]Center for Frontier Science, Chiba University, 1-33 Yayoi-cho, Inage-ku, Chiba 263-8522, Japan

Supporting Information

ABSTRACT: The electronic structures of the highest occupied molecular orbital (HOMO) or the HOMO-derived valence bands dominate the transport nature of positive charge carriers (holes) in organic semiconductors. In the present study, the valence-band structures of single-crystal pentacene and the temperature dependence of their energy−momentum dispersion relations are successfully demonstrated using angle-resolved ultraviolet photoelectron spectroscopy (ARUPS). For the shallowest valence band, the intermolecular transfer integral and effective mass of the holes are evaluated as 43.1 meV and 3.43 times the electron rest mass, respectively, at room temperature along the crystallographic direction for which the widest energy dispersion is expected. The temperature dependence of the ARUPS results reveals that the transfer integral values (hole effective mass) are enhanced (reduced) by ∼20% on cooling the sample to 110 K.

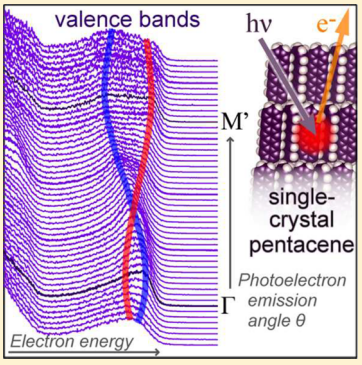

Charge carrier transport in semiconducting molecular solids is a central question in the pursuit of organic electronic devices with superior efficiencies. In particular, the mobility of charge carriers is regarded as a criterion not only of the appropriateness of a material for usage as a *good* semiconductor but also to distinguish the probable mechanism of transport, that is, bandlike or hopping transport. In this context, molecules exhibiting large mobility values attract attention from the viewpoints of both fundamental science and device applications. Moreover, because the molecular solids are constructed with weak van der Waals bonding, the charge carriers inside the solids generally undergo strong coupling with intra- and intermolecular vibrations. Accordingly, knowledge about the temperature dependence of the electronic structures is essential to clearly define the transport nature of the charge carriers as Holstein−Peierls-type small polarons in organic semiconducting materials.[1−6]

The present target molecule pentacene ($C_{22}H_{14}$) is one of the most well-studied organic semiconductor materials. Significantly large mobility values of the positive charges (holes) were reported in thin-film (1.5 $cm^2V^{-1}s^{-1}$)[7] and single-crystal (over 10 $cm^2V^{-1}s^{-1}$)[8] phases of pentacene, implying that the transport mechanism should be interpreted as bandlike rather than intermolecular hopping. As the electronic origin of the transport behavior, valence bands showing energy−momentum ($E-K$) dispersion relations have been proven on thin-film samples of pentacene using angle-resolved ultraviolet photoelectron spectroscopy (ARUPS).[9−13] Although such information on the band structures provides a fundamental basis for the transport nature,[14,15] it is generally not sufficient for comprehensive reproduction of the experimental values of charge-carrier mobility in thin-film devices because of strong disturbances in device performance by structural imperfections, such as grain boundaries.[16−18] Therefore, single crystals with minimized structural imperfections are suitable benchmarks for relating electronic structures directly with the electric responses exhibited by actual devices.

For single crystals of pentacene, many studies have estimated the charge-carrier mobility in field-effect transistor (FET) devices, with reported values of as great as 5 $cm^2V^{-1}s^{-1}$.[19−29] Moreover, theoretical calculations have predicted the formation of widely dispersed valence band derived from the highest occupied molecular orbital (HOMO).[30−32] However, although experimental characterization of the valence bands of the pentacene single crystal (Pn-SC) has been attempted,[33−35] the $E-K$ dispersion structures have not yet been observed experimentally. One reason for this situation is ascribed to the experimental difficulty of so-called "sample charging", which

Received: January 11, 2017
Accepted: February 27, 2017
Published: February 27, 2017

DOI: 10.1021/acs.jpclett.7b00082
J. Phys. Chem. Lett. 2017, 8, 1259−1264

commonly hinders accurate characterization by standard photoelectron spectroscopy techniques on single-crystal samples of organic semiconductors. This problem can be overcome with the assistance of enhanced photoconductivity under laser light illumination during photoelectron spectroscopy measurements, and the valence-band dispersion structures of the single crystal samples of several organic semiconductor materials have been successfully resolved in this way.[36−41] For the Pn-SC, fine analyses of inner-shell electronic states have recently been accomplished by means of photoconductivity-assisted high-resolution X-ray photoelectron spectroscopy (XPS).[42] Nevertheless, the $E-K$ dispersion of the valence bands has not yet been resolved by ultraviolet photoelectron spectroscopy experiments using standard excitation photon energies (e.g., 21.2 eV), even with the assistance of enhanced photoconductivity.

In this study, we successfully demonstrated the valence-band dispersion structures of the Pn-SC for the first time using photoconductivity-assisted ARUPS. Adopting low-energy (10 eV) photons as the excitation source enabled us to unveil the "bulk" band beneath the surface. The $E-K$ dispersion of the valence band was clearly resolved along the crystallographic direction for which the widest bandwidth has been theoretically predicted. In addition, the evolution of the valence-band structures upon cooling the sample temperature from room temperature to 110 K was also examined. The transfer integral and effective mass values for the conducting holes were revealed at these temperatures based on the present experimental results.

Single-crystal samples of pentacene were produced using previously described procedures.[34] Quasi-parallelogram-shaped plates (ca. 3 mm × 2 mm) of Pn-SCs were selected and attached to pieces of conductive carbon tape. Subsequently, silver paste was added at the peripheries of the crystals for good electrical contact. The surface index of the present sample was identified as (001) face by grazing incidence X-ray diffraction (GIXD) analysis at BL-46XU of SPring-8.[43] The orientation of the crystal lattice of the Pn-SC sample was determined by the anisotropic character of the crystal shape,[44] as illustrated in Figure 1b. Thus a slight misalignment of the sample azimuthal angle in the range of ±5° was inevitable, which may result in deviation of the reciprocal lattice point by ∼0.5 nm^{-1} at the boundary of the surface Brillouin zone (SBZ). Because the Pn-SC samples were exposed to ambient air for at least for 1 h and used as-is for ARUPS measurements, oxide species of a few percent population were likely formed at the crystal surface.[42,45]

ARUPS measurements were carried out at BL7U in UVSOR, IMS.[47] In the present work, the excitation photon energy was set at 10 eV. The probing depth of these measurements is expected to be deeper than the layer distance of the Pn-SC (1.41 nm)[46] because of the relatively long inelastic mean path (∼2 nm) of electrons of their kinetic energy <10 eV.[48−50] The photoelectron emission angle was varied along the Γ−M′ direction of the Pn-SC (Figure 1c), for which the widest energy dispersion has been theoretically predicted.[30] The sample was illuminated by continuous wave laser (405 nm, 30 mW) to relieve positive charging of the sample surface after photoelectron ejection.[36] The sample temperature without any intentional heating or cooling was 309 K, which we define as room temperature (RT) in this work. The sample was slowly cooled (approximately −1 K per 3 min) to trace the temperature dependence of the valence-band structures.

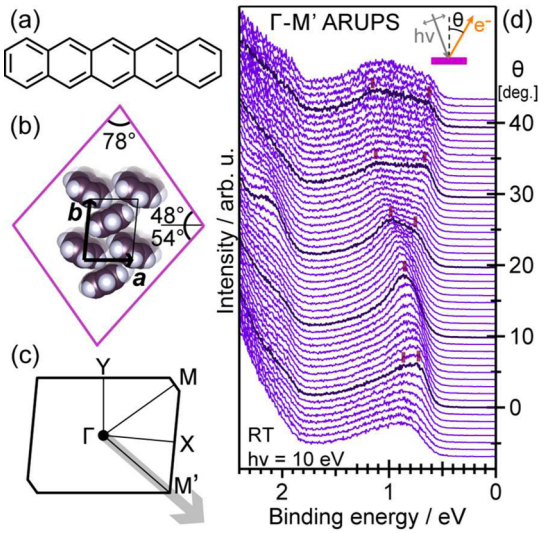

Figure 1. (a) Molecular structure of pentacene. (b) Schematic illustration of the molecular arrangement and unit cell of the PnSC (001) surface[46] with the typical parallelogram-shape of the Pn-SCs.[44] (c) Surface Brillouin zone of Pn-SC. The direction of the ARUPS measurements is indicated by the gray arrow. (d) ARUPS spectra of Pn-SC taken toward the Γ−M′ direction at RT. The vertical bars are guides for the eyes to indicate the peak positions of spectral components. The measurement geometry is illustrated in the inset.

Figure 1d shows ARUPS spectra of the Pn-SC taken at RT. The electron emission angles θ of 0° and ∼33° correspond to the Γ and M′ points in the SBZ, respectively. The abscissa is taken on an electron binding energy (BE) scale with respect to the Fermi level. Spectral profiles in the BE range of 0.5−1.5 eV, which are attributed to the valence band (highest occupied states) of the Pn-SC, exhibit characteristic transformations with respect to θ. In the normal emission condition (θ = 0°), two spectral components are resolved in close proximity to each other at BEs of <1 eV. By changing the emission angle, these components coalesce at around θ = 10°, split into two again by θ = 20°, and are further separated at larger θ. This variation represents the energy dispersion of the valence bands of the Pn-SC.

The ARUPS spectra of Figure 1d are represented on the $E-K_{\parallel}$ plane ($K_{\parallel}$ is the surface parallel component of the electron wavenumber) as shown in Figure 2a, where the electronic band structures are replicated as an undulation of the photoelectron intensity. The shape of the valence-band structures revealed by ARUPS measurements excellently reproduces the theoretical prediction.[30] Notably, the trend of the present dispersion relation, namely, the expansion of the energy split of the two bands when moving toward the edge of the SBZ along its diagonal direction, is in contrast with that of the thin-film phase of pentacene.[11]

The $E-K_{\parallel}$ dispersion relations of the Pn-SC valence bands were mapped as plotted in Figure 2b in which the energetic positions are determined through curve fitting of the individual ARUPS spectra corresponding to the respective θ (for details, see Supporting Information Figure S1). At the Γ point, the spectra in the valence-band region are resolved into three spectral components. The upper two components are attributed to the two valence bands originating from the HOMOs of the two pentacene molecules in the unit cell of the Pn-SC, whereas the third component of a dispersionless character may be ascribed to inelastic scattering of photo-

DOI: 10.1021/acs.jpclett.7b00082
J. Phys. Chem. Lett. 2017, 8, 1259−1264

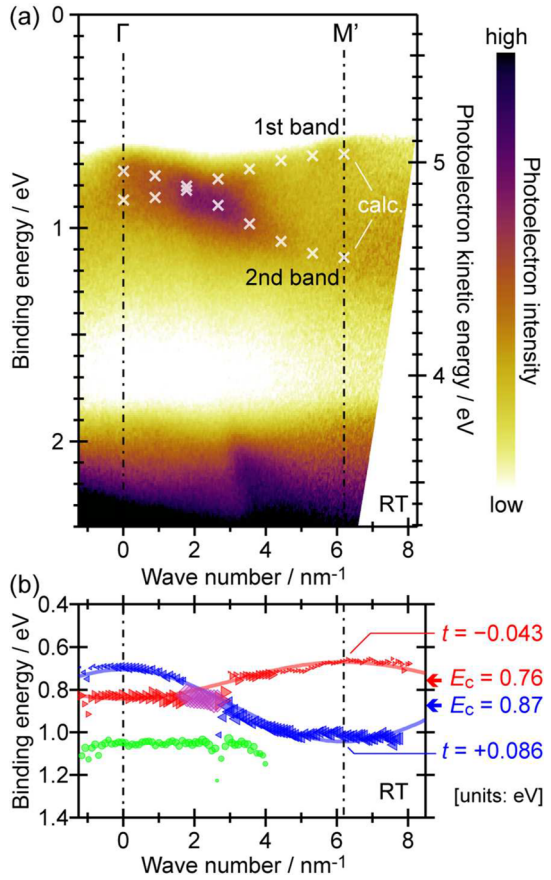

Figure 2. (a) Γ−M′ ARUPS spectral image taken at RT mapped on the $E-K_{\parallel}$ plane. The band calculation results[30] are also plotted as cross marks. (b) Binding energy positions of the three valence-band components derived through least-squares fitting of the ARUPS spectra plotted as a function of the electron wavenumber parallel to the surface. The sizes of the symbols represent the intensities of the respective spectral components. The 1D tight-binding (1D-TB) fitting curves for the first and second valence bands are shown as thick lines.

electrons by impurities.[36,39] The $E-K$ dispersion of the first and second bands can be reproduced well by a simple one-dimensional tight-binding (1D-TB) approximation as

$$E(K) = E_c + 2t\cos[dK] \quad (1)$$

where E_c is a BE position of the band center, t is the transfer integral, and d is the distance to the $(1\bar{1}0)$ lattice point. The E_c and t values, estimated by using the lattice constant reported by Mattheus et al.,[46] are listed in Table 1. It has to be noted that these values are derived solely from curvatures of the 2D valence bands toward the steepest direction (the "$-xy$" component) and thus may contain some uncertainness in the absolute values. The first and second bands approach closest to the Fermi level at the M′ and Γ points, respectively, and the BE of the first band top is even smaller than that of the second band, as indicated in Table 1. Hence, the valence band maximum (VBM) is located at the M′ point rather than Γ, which is also in agreement with the theoretical work.[30]

Figure 3 shows the ARUPS spectra of the Pn-SC taken at lower temperatures. The overall appearance of the spectral images does not change significantly, which corroborates the absence of notable phase transitions of the Pn-SC in the present temperature range.[46] It is interesting to note that the present $E-K_{\parallel}$ dispersion width and behaviors exhibit close resemblance to those of the "bulk-phase" pentacene monolayer (see Supporting Information Figure S2).[10] Using the 1D-TB approximation, E_c and t for the first and second bands were evaluated, as listed in Table 1, where the lattice constant values at each temperature are approximated by simple linear interpolation of the reported crystallographic data.[46] The VBM position is still at the M′ point of the first band at the lower temperatures. This finding indicates that when the charge carrier density is not too high, conductive holes injected from electrodes into the Pn-SC are located in the first valence band with a narrower energetic dispersion rather than in the second band with a wider dispersion.

Whether charge-carrier transport in the Pn-SC is bandlike or hopping transport has been under debate. One necessary condition for bandlike transport is $|4t| > k_BT$ (k_B: Boltzmann constant; T: temperature), which is fulfilled at RT in the present case even for the narrower first band. In the bandlike transport framework, the mobility of a charge carrier is given as a function of its effective mass m^*. From the energy−time uncertainty relation, the lowest limit of the drift mobility μ_D of the charge carriers is given by their m^* as[51]

$$\mu_D \gtrsim 20 \times (300/T) \times (m^*/m_0)^{-1}\ [\mathrm{cm^2V^{-1}s^{-1}}] \quad (2)$$

where m_0 is the electron rest mass and the temperature T is given in Kelvins. In the present case, the m^* value of the holes (m_h^*) derived from the curvature at the top of each band and the lowest limits of μ_D are summarized in Table 1.

It is noteworthy that the field-effect mobility values of the Pn-SC reported so far do not exceed the theoretical lowest limits expected from inequality 2, as also listed in the Supporting Information Table S1. This is in contrast with the case of rubrene single crystals where the experimental mobility[52] surpasses the theoretical lower limit.[36] In this context, it is worth examining the validity of the hopping transport. In fact, based on their systematic Hall-effect measurements, Uemura et al. proposed "decoherence" of the conducting holes in Pn-SCs, namely, that the transport mechanism cannot be simply explained as bandlike transport but some contribution from hopping transport has to be taken into consideration.[26]

Table 1. Band Center Positions (E_c), Transfer Integrals (t), and Energy Positions at the Band Tops ($E_{M'}$ and E_Γ, respectively), hole Effective Mass (m_h^*), Lower Limit of the Drift Mobility Values (μ_D), and Upper Limit of the Hopping Mobility Values (μ_{ET}), of the First and Second Valence Bands of the Pn-SC Derived from the Present Temperature-Dependent ARUPS Results

	E_c/eV		t/meV		$E_{M'}$/eV	E_Γ/eV	m_h^*/m_0		μ_D/cm^{2}V^{-1}s^{-1}		μ_{ET}/cm^{2}V^{-1}s^{-1}	
temperature	first	second	first	second	first	second	first	second	first	second	first	second
RT	0.760	0.866	−43.1	+86.4	0.674	0.694	3.43	1.71	5.7	11.4	2.8	11.4
212 K	0.668	0.800	−45.7	+85.1	0.576	0.630	3.26	1.75	8.7	16.2	3.6	12.4
110 K	0.684	0.808	−53.1	+88.2	0.578	0.632	2.81	1.70	19.3	32.0	3.3	9.2

DOI: 10.1021/acs.jpclett.7b00082
J. Phys. Chem. Lett. 2017, 8, 1259−1264

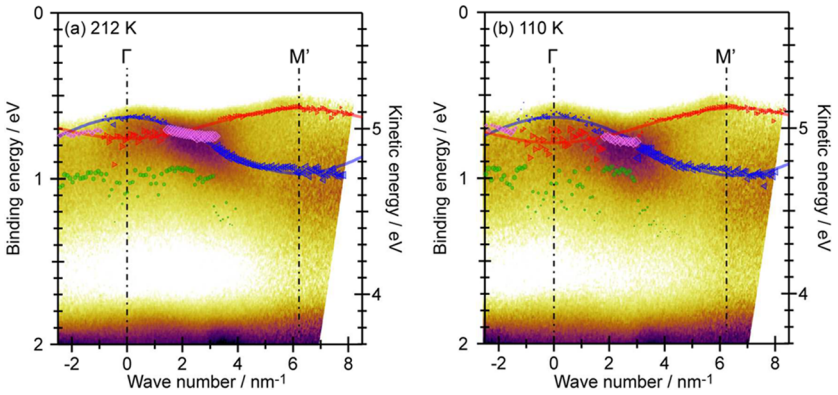

Figure 3. Γ-M′ ARUPS spectral images taken at (a) 212 and (b) 110 K mapped on the $E-K_{\parallel}$ plane. The energy positions of the valence-band components derived from the ARUPS data and the corresponding 1D-TB fitting curves are overlaid on the images.

The upper limit of the hopping mobility μ_{ET} in molecular solids can be formulated based on the Marcus rate equation for electron transfer as[53]

$$\mu_{ET} = (eL^2/k_BT)k_{ET} \quad (3)$$

$$k_{ET} = 2\pi t^2/\hbar \times (4\pi\lambda k_BT)^{-1/2} \times \exp[-\lambda/k_BT] \quad (4)$$

where e is the elementary charge, L is the distance between adjacent molecules (hopping length), k_{ET} is the electron transfer rate constant, and λ is the reorganization energy. The μ_{ET} values for positive charge carriers along the Γ-M′ direction of the Pn-SC were evaluated, as listed in Table 1, where $L = d/2$ was applied for the present case and λ was taken from experimental values for thin-film phase pentacene.[54,55] These values are fairly consistent with the reported *good* field-effect mobility values (~2 $cm^2V^{-1}s^{-1}$)[20,22,23,26] of Pn-SC FETs, although the recently reported *best* experimental results (~5 $cm^2V^{-1}s^{-1}$)[27−29] are beyond these limits. The present results also imply that the conduction mechanism in the Pn-SC cannot be comprehended within either the bandlike or hopping transport framework but that both take part in the charge-carrier transport behavior.

Finally, we discuss the possible distinction between surface and bulk electronic bands. On the single crystal of tetracene ($C_{18}H_{10}$), a smaller member of the polyacene family, structural relaxation at the top surface layer was reported.[56] Accordingly, the opposite valence-band dispersion behavior was predicted by calculation for the surface-crystalline layer and the bulk; namely, the two surface valence bands split widely at the Γ point and approach each other along the diagonal direction of the SBZ. As mentioned above, the probing depth of the present measurements is deeper than the monomolecular height of pentacene, and thus the ARUPS results in this work mainly represent the bulk band structures of the Pn-SC. It is noteworthy that the valence-band dispersion disappeared for surface-sensitive ARUPS measurements on the Pn-SC samples at higher photon energies (e.g., $h\nu$ = 21.2 eV). The absence of the surface-band dispersion may be ascribed to the presence of surface impurities that disturb the coherence of the charge carriers at the surface of the Pn-SC. Attempts to characterize the "clean surface" of the PnSC are underway to resolve the surface valence-band structures using ARUPS measurements.

In conclusion, the electronic band structures of the Pn-SC and their dependence on temperature were experimentally demonstrated by ARUPS. Two valence bands, which disperse in opposite directions, were clearly resolved. The VBM was revealed to be at the border of the SBZ on one valence band with a narrower $E-K_{\parallel}$ dispersion rather than at the Γ point on the other band with a wider dispersion. The transfer integral and effective mass values for the positive charge carriers at the VBM were evaluated under the 1D-TB assumption as 43.1 meV and $3.41m_0$, respectively, at RT, whereas these values increased and decreased by ~20%, respectively, at 110 K. The former effective mass value corresponds to the lowest limit of the hole mobility of 5.7 $cm^2V^{-1}s^{-1}$ at RT. This value suggests that the simple bandlike transport assumption may overestimate the practical field-effect mobility of Pn-SC FETs. On the contrary, the highest limit of hopping mobility at RT is expected to be 2.8 $cm^2V^{-1}s^{-1}$, which is insufficient to explain recently reported experimental field-effect mobility values. Accordingly, the present results suggest that the charge-carrier conduction mechanism in Pn-SCs must be a hybrid case of bandlike and hopping transport frameworks.

■ ASSOCIATED CONTENT

Supporting Information

The Supporting Information is available free of charge on the ACS Publications website at DOI: 10.1021/acs.jpclett.7b00082.

Procedures for peak separation of the ARUPS spectra, comparison to the previous ARUPS data of the "bulk phase" pentacene film, and comparison to the experimental mobility values (PDF)

■ AUTHOR INFORMATION

Corresponding Author

*E-mail: nkym@rs.tus.ac.jp.

ORCID

Yasuo Nakayama: 0000-0001-5014-6858

Notes

The authors declare no competing financial interest.

■ ACKNOWLEDGMENTS

We thank Dr. Takuya Hosokai of National Institute of Advanced Industrial Science and Technology, Dr. Tomoyuki Koganezawa of Japan Synchrotron Radiation Research Institute (JASRI), and Mr. Ryohei Tsuruta of Tokyo University of Science for their help on the GIXD measurement that was performed under approval of JASRI [2015A1685]. The ARUPS experiments were conducted as the Joint Studies Programs [26-530, 26-812, and 27-530] of IMS. Financial supports from JSPS-KAKENHI Grant Numbers JP15H05498, JP16K14102,

DOI: 10.1021/acs.jpclett.7b00082
J. Phys. Chem. Lett. 2017, 8, 1259−1264

and JP25288114, G-COE/TAKUETSU Programs of Chiba University [G-3, MEXT], Izumi Science and Technology Foundation, and JGC-S Scholarship Foundation are gratefully acknowledged. This work was also partially supported by the Futaba Electronics Memorial Foundation.

REFERENCES

(1) Coropceanu, V.; Li, Y.; Yi, Y.; Zhu, L.; Brédas, J.-L. Intrinsic Charge Transport in Single Crystals of Organic Molecular Semiconductors: A Theoretical Perspective. *MRS Bull.* **2013**, *38*, 57−64.
(2) Fratini, S.; Ciuchi, S. Dynamical Mean-Field Theory of Transport of Small Polarons. *Phys. Rev. Lett.* **2003**, *91*, 256403.
(3) Hannewald, K.; Stojanović, V. M.; Schellekens, J. M. T.; Bobbert, P. A.; Kresse, G.; Hafner, J. Theory of Polaron Bandwidth Narrowing in Organic Molecular. *Phys. Rev. B: Condens. Matter Mater. Phys.* **2004**, *69*, 075211.
(4) Ortmann, F.; Bechstedt, F.; Hannewald, K. Theory of Charge Transport in Organic Crystals: Beyond Holstein's Small-Polaron Model. *Phys. Rev. B: Condens. Matter Mater. Phys.* **2009**, *79*, 235206.
(5) Blülle, B.; Troisi, A.; Häusermann, R.; Batlogg, B. Charge Transport Perpendicular to the High Mobility Plane in Organic Crystals: Bandlike Temperature Dependence Maintained despite Hundredfold Anisotropy. *Phys. Rev. B: Condens. Matter Mater. Phys.* **2016**, *93*, 035205.
(6) Fratini, S.; Mayou, D.; Ciuchi, S. The Transient Localization Scenario for Charge Transport in Crystalline Organic Materials. *Adv. Funct. Mater.* **2016**, *26*, 2292−2315.
(7) Lin, Y.-Y.; Gundlach, D. J.; Nelson, S. F.; Jackson, T. N. Stacked Pentacene Layer Organic Thin-Film Transistors with Improved Characteristics. *IEEE Electron Device Lett.* **1997**, *18*, 606−608.
(8) Jurchescu, O. D.; Baas, J.; Palstra, T. T. M. Effect of Impurities on the Mobility of Single Crystal Pentacene. *Appl. Phys. Lett.* **2004**, *84*, 3061−3063.
(9) Koch, N.; Vollmer, A.; Salzmann, I.; Nickel, B.; Weiss, H.; Rabe, J. Evidence for Temperature-Dependent Electron Band Dispersion in Pentacene. *Phys. Rev. Lett.* **2006**, *96*, 156803.
(10) Kakuta, H.; Hirahara, T.; Matsuda, I.; Nagao, T.; Hasegawa, S.; Ueno, N.; Sakamoto, K. Electronic Structures of the Highest Occupied Molecular Orbital Bands of a Pentacene Ultrathin Film. *Phys. Rev. Lett.* **2007**, *98*, 247601.
(11) Ohtomo, M.; Suzuki, T.; Shimada, T.; Hasegawa, T. Band Dispersion of Quasi-Single Crystal Thin Film Phase Pentacene Monolayer Studied by Angle-Resolved Photoelectron Spectroscopy. *Appl. Phys. Lett.* **2009**, *95*, 123308.
(12) Hatch, R.; Huber, D.; Höchst, H. HOMO Band Structure and Anisotropic Effective Hole Mass in Thin Crystalline Pentacene Films. *Phys. Rev. B: Condens. Matter Mater. Phys.* **2009**, *80*, 081411.
(13) Ciuchi, S.; Hatch, R.; Höchst, H.; Faber, C.; Blase, X.; Fratini, S. Molecular Fingerprints in the Electronic Properties of Crystalline Organic Semiconductors: From Experiment to Theory. *Phys. Rev. Lett.* **2012**, *108*, 256401.
(14) Ueno, N.; Kera, S. Electron Spectroscopy of Functional Organic Thin Films: Deep Insights into Valence Electronic Structure in Relation to Charge Transport Property. *Prog. Surf. Sci.* **2008**, *83*, 490−557.
(15) Hatch, R. C.; Huber, D. L.; Höchst, H. Electron-Phonon Coupling in Crystalline Pentacene Films. *Phys. Rev. Lett.* **2010**, *104*, 047601.
(16) Kelley, T. W.; Frisbie, C. D. Gate Voltage Dependent Resistance of a Single Organic Semiconductor Grain Boundary. *J. Phys. Chem. B* **2001**, *105*, 4538−4540.
(17) Verlaak, S.; Arkhipov, V.; Heremans, P. Modeling of Transport in Polycrystalline Organic Semiconductor Films. *Appl. Phys. Lett.* **2003**, *82*, 745−747.
(18) Nakamura, M.; Goto, N.; Ohashi, N.; Sakai, M.; Kudo, K. Potential Mapping of Pentacene Thin-Film Transistors Using Purely Electric Atomic-Force-Microscope Potentiometry. *Appl. Phys. Lett.* **2005**, *86*, 122112.
(19) Butko, V. Y.; Chi, X.; Lang, D. V.; Ramirez, A. P. Field-Effect Transistor on Pentacene Single Crystal. *Appl. Phys. Lett.* **2003**, *83*, 4773−4775.
(20) Goldmann, C.; Haas, S.; Krellner, C.; Pernstich, K. P.; Gundlach, D. J.; Batlogg, B. Hole Mobility in Organic Single Crystals Measured by A "flip- Crystal" field-Effect Technique. *J. Appl. Phys.* **2004**, *96*, 2080−2086.
(21) Takeya, J.; Nishikawa, T.; Takenobu, T.; Kobayashi, S.; Iwasa, Y.; Mitani, T.; Goldmann, C.; Krellner, C.; Batlogg, B. Effects of Polarized Organosilane Self-Assembled Monolayers on Organic Single-Crystal Field-Effect Transistors. *Appl. Phys. Lett.* **2004**, *85*, 5078−5080.
(22) Lee, J. Y.; Roth, S.; Park, Y. W. Anisotropic Field Effect Mobility in Single Crystal Pentacene. *Appl. Phys. Lett.* **2006**, *88*, 252106.
(23) Reese, C.; Chung, W. J.; Ling, M. M.; Roberts, M.; Bao, Z. High-Performance Microscale Single-Crystal Transistors by Lithography on an Elastomer Dielectric. *Appl. Phys. Lett.* **2006**, *89*, 202108.
(24) Takenobu, T.; Watanabe, K.; Yomogida, Y.; Shimotani, H.; Iwasa, Y. Effect of Postannealing on the Performance of Pentacene Single-Crystal Ambipolar Transistors. *Appl. Phys. Lett.* **2008**, *93*, 073301.
(25) Kimura, Y.; Niwano, M.; Ikuma, N.; Goushi, K.; Itaya, K. Organic Field Effect Transistor Using Pentacene Single Crystals Grown by a Liquid-Phase Crystallization Process. *Langmuir* **2009**, *25*, 4861−4863.
(26) Uemura, T.; Yamagishi, M.; Soeda, J.; Takatsuki, Y.; Okada, Y.; Nakazawa, Y.; Takeya, J. Temperature Dependence of the Hall Effect in Pentacene Field-Effect Transistors: Possibility of Charge Decoherence Induced by Molecular Fluctuations. *Phys. Rev. B: Condens. Matter Mater. Phys.* **2012**, *85*, 035313.
(27) Takeyama, Y.; Ono, S.; Matsumoto, Y. Organic Single Crystal Transistor Characteristics of Single-Crystal Phase Pentacene Grown by Ionic Liquid-Assisted Vacuum Deposition. *Appl. Phys. Lett.* **2012**, *101*, 083303.
(28) Arabi, S. A.; Dong, J.; Mirza, M.; Yu, P.; Wang, L.; He, J.; Jiang, C. Nanoseed Assisted PVT Growth of Ultrathin 2D Pentacene Molecular Crystal Directly onto SiO_2 Substrate. *Cryst. Growth Des.* **2016**, *16*, 2624−2630.
(29) Dong, J.; Yu, P.; Arabi, S. A.; Wang, J.; He, J.; Jiang, C. Enhanced Mobility in Organic Field-Effect Transistors due to Semiconductor/dielectric iInterface Control and Very Thin Single Crystal. *Nanotechnology* **2016**, *27*, 275202.
(30) Yoshida, H.; Sato, N. Crystallographic and Electronic Structures of Three Different Polymorphs of Pentacene. *Phys. Rev. B: Condens. Matter Mater. Phys.* **2008**, *77*, 235205.
(31) Haddon, R. C.; Chi, X.; Itkis, M. E.; Anthony, J. E.; Eaton, D. L.; Siegrist, T.; Mattheus, C. C.; Palstra, T. T. M. Band Electronic Structure of One- and Two-Dimensional Pentacene Molecular Crystals. *J. Phys. Chem. B* **2002**, *106*, 8288−8292.
(32) Cheng, Y. C.; Silbey, R. J.; da Silva Filho, D. A.; Calbert, J. P.; Cornil, J.; Brédas, J. L. Three-Dimensional Band Structure and Bandlike Mobility in Oligoacene Single Crystals: A Theoretical Investigation. *J. Chem. Phys.* **2003**, *118*, 3764−3774.
(33) Vollmer, A.; Jurchescu, O. D.; Arfaoui, I.; Salzmann, I.; Palstra, T. T. M.; Rudolf, P.; Niemax, J.; Pflaum, J.; Rabe, J. P.; Koch, N. The Effect of Oxygen Exposure on Pentacene Electronic Structure. *Eur. Phys. J. E: Soft Matter Biol. Phys.* **2005**, *17*, 339−343.
(34) Nakayama, Y.; Uragami, Y.; Yamamoto, M.; Machida, S.; Kinjo, H.; Mase, K.; Koswattage, K. R.; Ishii, H. Determination of the Highest Occupied Molecular Orbital Energy of Pentacene Single Crystals by Ultraviolet Photoelectron and Photoelectron Yield Spectroscopies. *Jpn. J. Appl. Phys.* **2014**, *53*, 01AD03.
(35) Yamamoto, M.; Nakayama, Y.; Uragami, Y.; Kinjo, H.; Mizuno, Y.; Mase, K.; Koswattage, K. R.; Ishii, H. Electronic Structures of a Well-Dened Organic Hetero-Interface: C60 on Pentacene Single Crystal. *e-J. Surf. Sci. Nanotechnol.* **2015**, *13*, 59−64.
(36) Machida, S.; Nakayama, Y.; Duhm, S.; Xin, Q.; Funakoshi, A.; Ogawa, N.; Kera, S.; Ueno, N.; Ishii, H. Highest-Occupied-Molecular-Orbital Band Dispersion of Rubrene Single Crystals as Observed by

DOI: 10.1021/acs.jpclett.7b00082
J. Phys. Chem. Lett. 2017, 8, 1259−1264

Angle-Resolved Ultraviolet Photoelectron Spectroscopy. *Phys. Rev. Lett.* **2010**, *104*, 156401.
(37) Ding, H.; Reese, C.; Mäkinen, A. J.; Bao, Z.; Gao, Y. Band Structure Measurement of Organic Single Crystal with Angle-Resolved Photoemission. *Appl. Phys. Lett.* **2010**, *96*, 222106.
(38) Nakayama, Y.; Uragami, Y.; Machida, S.; Koswattage, K. R.; Yoshimura, D.; Setoyama, H.; Okajima, T.; Mase, K.; Ishii, H. Full Picture of the Valence Band Structure of Rubrene Single Crystals Probed by Angle-Resolved and Excitation Energy Dependent Photoelectron Spectroscopy. *Appl. Phys. Express* **2012**, *5*, 111601.
(39) Vollmer, A.; Ovsyannikov, R.; Gorgoi, M.; Krause, S.; Oehzelt, M.; Lindblad, A.; Mårtensson, N.; Svensson, S.; Karlsson, P.; Lundvuist, M.; et al. Two Dimensional Band Structure Mapping of Organic Single Crystals Using the New Generation Electron Energy Analyzer ARTOF. *J. Electron Spectrosc. Relat. Phenom.* **2012**, *185*, 55−60.
(40) Xin, Q.; Duhm, S.; Bussolotti, F.; Akaike, K.; Kubozono, Y.; Aoki, H.; Kosugi, T.; Kera, S.; Ueno, N. Accessing Surface Brillouin Zone and Band Structure of Picene Single Crystals. *Phys. Rev. Lett.* **2012**, *108*, 226401.
(41) Nakayama, Y.; Niederhausen, J.; Machida, S.; Uragami, Y.; Kinjo, H.; Vollmer, A.; Rabe, J. P.; Koch, N.; Ishii, H. Valence Band Structure of Rubrene Single Crystals in Contact with an Organic Gate Dielectric. *Org. Electron.* **2013**, *14*, 1825−1832.
(42) Nakayama, Y.; Uragami, Y.; Yamamoto, M.; Yonezawa, K.; Mase, K.; Kera, S.; Ishii, H.; Ueno, N. High-Resolution Core-Level Photoemission Measurements on the Pentacene Single Crystal Surface Assisted by Photoconduction. *J. Phys.: Condens. Matter* **2016**, *28*, 094001.
(43) Nakayama, Y.; Mizuno, Y.; Hosokai, T.; Koganezawa, T.; Tsuruta, R.; Hinderhofer, A.; Gerlach, A.; Broch, K.; Belova, V.; Frank, H.; et al. Epitaxial Growth of an Organic P-N Heterojunction: C60 on Single-Crystal Pentacene. *ACS Appl. Mater. Interfaces* **2016**, *8*, 13499−13505.
(44) Jo, S.; Takenaga, M. Morphologies of Pentacene Crystals Obtained by Physical Vapor Growth Technique. *Jpn. J. Appl. Phys.* **2010**, *49*, 078002.
(45) Mizuno, Y.; Yamamoto, M.; Kinjo, H.; Mase, K.; Ishii, H.; Okudaira, K. K.; Yoshida, H.; Nakayama, Y. Effects of the Ambient Exposure on the Electronic States of the Clean Surface of the Pentacene Single Crystal. *Mol. Cryst. Liq. Cryst.* **2017**, In press.
(46) Mattheus, C. C.; Dros, A. B.; Baas, J.; Meetsma, A.; de Boer, J. L.; Palstra, T. T. Polymorphism in Pentacene. *Acta Crystallogr., Sect. C: Cryst. Struct. Commun.* **2001**, *57*, 939−941.
(47) Kimura, S.-I.; Ito, T.; Sakai, M.; Nakamura, E.; Kondo, N.; Horigome, T.; Hayashi, K.; Hosaka, M.; Katoh, M.; Goto, T.; et al. SAMRAI: A Novel Variably Polarized Angle-Resolved Photoemission Beamline in the VUV Region at UVSOR-II. *Rev. Sci. Instrum.* **2010**, *81*, 053104.
(48) Seah, M. P.; Dench, W. A. Quantitative Electron Spectroscopy of Surfaces: A Standard Data Base for Electron Inelastic Mean Free Paths in Solids. *Surf. Interface Anal.* **1979**, *1*, 2−11.
(49) Bussolotti, F.; Kera, S.; Kudo, K.; Kahn, A.; Ueno, N. Gap States in Pentacene Thin Film Induced by Inert Gas Exposure. *Phys. Rev. Lett.* **2013**, *110*, 267602.
(50) Ozawa, Y.; Nakayama, Y.; Machida, S.; Kinjo, H.; Ishii, H. Maximum Probing Depth of Low-Energy Photoelectrons in an Amorphous Organic Semiconductor Film. *J. Electron Spectrosc. Relat. Phenom.* **2014**, *197*, 17−21.
(51) Fröhlich, H.; Sewell, G. Electric Conduction in Semiconductors. *Proc. Phys. Soc., London* **1959**, *74*, 643−647.
(52) Takeya, J.; Yamagishi, M.; Tominari, Y.; Hirahara, R.; Nakazawa, Y.; Nishikawa, T.; Kawase, T.; Shimoda, T.; Ogawa, S. Very High-Mobility Organic Single-Crystal Transistors with in-Crystal Conduction Channels. *Appl. Phys. Lett.* **2007**, *90*, 102120.
(53) Kera, S.; Yamane, H.; Ueno, N. First-Principles Measurements of Charge Mobility in Organic Semiconductors: Valence Hole−vibration Coupling in Organic Ultrathin Films. *Prog. Surf. Sci.* **2009**, *84*, 135−154.
(54) Yamane, H.; Nagamatsu, S.; Fukagawa, H.; Kera, S.; Friedlein, R.; Okudaira, K. K.; Ueno, N. Hole-Vibration Coupling of the Highest Occupied State in Pentacene Thin Films. *Phys. Rev. B: Condens. Matter Mater. Phys.* **2005**, *72*, 153412.
(55) Kera, S.; Hosoumi, S.; Sato, K.; Fukagawa, H.; Nagamatsu, S. I.; Sakamoto, Y.; Suzuki, T.; Huang, H.; Chen, W.; Wee, A. T. S.; et al. Experimental Reorganization Energies of Pentacene and Perfluoropentacene: Effects of Perfluorination. *J. Phys. Chem. C* **2013**, *117*, 22428−22437.
(56) Morisaki, H.; Koretsune, T.; Hotta, C.; Takeya, J.; Kimura, T.; Wakabayashi, Y. Large Surface Relaxation in the Organic Semiconductor Tetracene. *Nat. Commun.* **2014**, *5*, 5400.

DOI: 10.1021/acs.jpclett.7b00082
J. Phys. Chem. Lett. 2017, 8, 1259−1264